Global Journal of Engineering and Technology Advances
eISSN: 2582-5003
Cross Ref DOI: 10.30574/gjeta
Journal homepage: https://gjeta.com/

(RESEARCH ARTICLE)

Check for updates

Analysis of coupling effects on hydraulic controlled 6 degrees of freedom parallel manipulator

P. O. Ogbobe [1,*] and C. N. Okoye [2]

[1] *Department of Information and Communication Technology, National Board for Technology Incubation, Abuja, Nigeria.*
[2] *Department of Science and Technical Education, Federal Ministry of Education, Abuja, Nigeria.*

Global Journal of Engineering and Technology Advances, 2022, 10(03), 026–031

Publication history: Received on 09 February 2022; revised on 12 March 2022; accepted on 14 March 2022

Article DOI: https://doi.org/10.30574/gjeta.2022.10.3.0051

Abstract

This paper presents an analysis of the coupling effects between degrees of freedom of a hydraulic controlled six DOF parallel manipulator. Based on the singular value decomposition to the properties of its joint space inverse mass matrix, the method is put forward to analyze coupling effects between degrees of freedom using a transformation matrix, the product of transposed Jabobian matrix and an orthogonal unitary matrix, of which each element represents decoupled modal space coordinates with respect to physical task space frame. The simulation results in frequency domain prove the theoretical analysis right. The analysis will provide useful information to mechanism and controller designer, to asses from concept the coupling effects between DOF in respect of the requirement for a particular application and also for the study on decoupling control strategies.

Keywords: 6 Degrees of freedom; Parallel manipulator; Singular value decomposition; Coupling effects; Orthogonal unitary matrix

1. Introduction

Six degrees of freedom parallel manipulator (6 DOF PM), like Stewart platform has many possible uses including flight simulation, machining, robotic assembly, vibration isolation, etc. Unlike the serial manipulators, it has better accuracy, large mechanical advantage, and higher payload to weight ratio and less sensitive to joint disturbances [1,2]. Disadvantages of the manipulator include smaller workspace, complex command and lower dexterity due to high coupling. In many applications requiring 6 DOF PM, the possibility of decoupling end effector motion has become a basic design criteria and this has led to extensive studies on coupling in 6 DOF PM by many researchers resulting to PM with decoupled structures [1,4]. Despite many solutions and methods provided on decoupling 6 DOF PM, it is far from being fully dynamically decoupled because, the motion freedom of the end effector is highly coupled due to its multi loop kinematics structure and a single axis motion in PM requires the coordination of all actuators, hence the highly coupled dynamic motion of manipulator [5,6,7].

The focus of this paper is on the analysis of the coupling effects between DOF of the PM based on the singular value decomposition to the properties of the joint space inverse mass matrix. The goal is to provide some useful information that will assist mechanism and controller designer to conceptually evaluate the coupling effects between DOF and how it affects the performance of the proposed manipulator and also for studies on decoupling control strategies based on the joint space inverse mass matrix.

* Corresponding author: P. O. Ogbobe
Department of Information and Communication Technology, National Board for Technology Incubation, Abuja, Nigeria.

The rest of the papers is organized as follows: theoretical analysis of coupling effects based on singular value decomposition (SVD) to the joint space inverse mass matrix will be presented in 2. In section 3 the dynamics of the hydraulics servo system will be discussed, section 4 will focus on simulation of the integrated dynamics model of the platform and analysis in frequency domain using Mathlab/Simulink tool box. Finally, we will conclude in section 5.

2. System Dynamics

The Stewart platform for our study is a six DOF closed kinematic chain mechanism with two bodies connected by the six extensible legs consisting of a fixed base {b} and a moveable platform {p} with six hydraulic actuators supporting it as shown in Fig.1. At neutral position the body axes {p} attached to the movable platform are parallel to and coincide with the inertial frame {b} fixed to the base with its origin at the geometric centre of the base platform.

Applying rigid body modeling theory in establishing the dynamic model of the parallel manipulator, we can make the following assumptions: (1) the moving platform and the fixed platform are rigid bodies. (2) The piston rod and cylinder are rigid bodies. (3) Hinges and other connectors are all rigid connectors with negligible masses. Based on the above stated assumptions, the system consists of 13 rigid bodies including 6 piston rods, 6 cylinders, and one moving platform [4]. The system dynamics can be expressed as:

$$\mathbf{M}_t(\bar{\mathbf{sx}})\ddot{\bar{\mathbf{x}}} + \mathbf{C}_t\left(\bar{\mathbf{sx}},\dot{\bar{\mathbf{x}}}\right)\dot{\bar{\mathbf{x}}} + \overline{\mathbf{G}}_t(\bar{\mathbf{sx}}) = \mathbf{J}_{l,x}^{\mathrm{T}}(\bar{\mathbf{sx}})\bar{\mathbf{f}}_a \qquad (1)$$

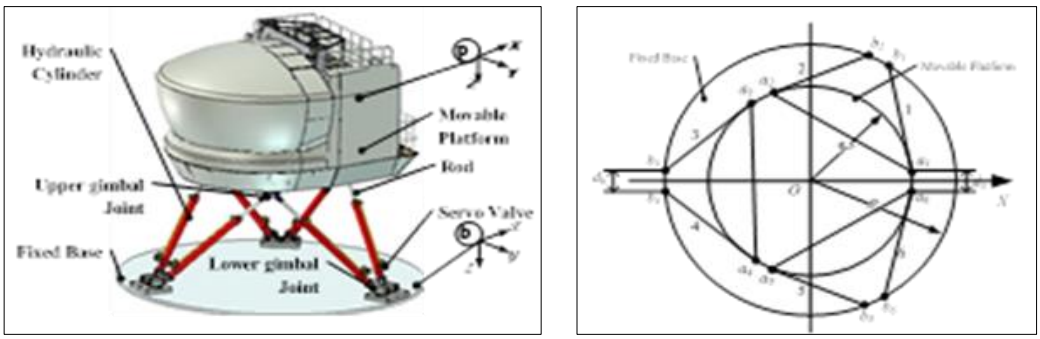

Figure 1 Schematic and top view of hydraulic controlled Parallel Manipulator

Where, $\bar{\mathbf{sx}} = [\mathrm{x} \quad \mathrm{y} \quad \mathrm{z} \quad \varphi \quad \theta \quad \psi]^{\mathrm{T}}$, is the 6×1 vector of the platform position with respect to the fixed base frame, and contains translation and angular motion velocity vectors respectively, and $\mathbf{M}_t(\bar{\mathbf{sx}})$ is a 6×6 mass matrix, $\mathbf{C}_t\left(\bar{\mathbf{sx}},\dot{\bar{\mathbf{x}}}\right)$ is 6×1 vector of centrifugal and Coriolis terms, $\mathbf{G}(\bar{\mathbf{sx}})$ is 6×1 vector of gravity terms, $\bar{\mathbf{f}}_{\mathrm{a}} = (f_{\mathrm{a1}} \quad f_{\mathrm{a2}} \quad \ldots \quad f_{\mathrm{a6}})^{\mathrm{T}}$, $\bar{\mathbf{f}}_{\mathrm{a}i}$ (i=1,...,6) is the i^{th} actuator output force, $\dot{\bar{\mathbf{x}}}$ and $\ddot{\bar{\mathbf{x}}}$ are the 6×1 platform velocity vector and acceleration vector respectively, and both contain translation and angular components. $\mathbf{J}_{lx}(\bar{\mathbf{sx}})$, is 6×6 Jacobian matrix relating the platform motion with respect to the actuators length changes in joint space. From (1), the coupling effects are from three terms: the mass matrix, the Coriolis /centrifugal and the gravitational, we obtained a simplified dynamics model neglecting Coriolis/centrifugal and gravity terms, gravity term to be compensated for while Coriolis/centrifugal will be treated as external disturbances in the Matlab/Simulink simulation model, (1) reduces to:

$$\mathbf{J}_{\mathrm{lx}}^{\mathrm{T}}\bar{\mathbf{f}}_a = \mathbf{M}_t\ddot{\bar{\mathbf{x}}} \qquad (2)$$

The actuator forces, $\bar{\mathbf{f}}_a$ will affect the platform coordinates, through the transposed Jacobian $\mathbf{J}_{\mathrm{lx}}^{\mathrm{T}}$, and the platform velocity will have to be projected along actuators by using $\mathbf{J}_{\mathbf{lx}}\dot{\bar{\mathbf{x}}} \approx \dot{\bar{\mathbf{l}}}$, $\dot{\bar{\mathbf{l}}}$ is the 6×1 velocity vector of the actuator length changes. The derivative of the velocity will give $\ddot{\bar{\mathbf{l}}} = \mathbf{J}_{\mathbf{lx}}.\ddot{\bar{\mathbf{X}}} + \left(\dot{\mathbf{J}}_{\mathbf{lx}}\dot{\mathbf{X}}\right)$, $\ddot{\bar{\mathbf{l}}}$ is the 6×1 acceleration vector of the actuator length changes. The term in the bracket represents the Coriolis/centripetal ignored in (1). Substituting $\mathbf{J}_{lx}\ddot{\bar{\mathbf{x}}} \approx \ddot{\bar{\mathbf{l}}}$, in (2) we have:

$$\mathbf{J_{lx}M_t^{-1}(sx)J_{lx}^T\bar{f}_a = \ddot{\bar{I}}} \quad (3)$$

Equation (3) is the inverse mass matrix in joint space, while $\mathbf{M_{act} = J_{lx}^{-1^T} M_t J_{lx}^{-1}}$, is the joint space mass matrix containing the platform pose $\bar{\mathbf{sx}}$ dependent Jacobian matrix and an almost constant platform mass matrix $\mathbf{M_t}$. This mass matrix $\left(\mathbf{M_{act}^{-1}}\right)$, is nonzero; it determines the coupling effects of the platform. It is symmetric, positive definite; the eigenvector matrix can be made unitary. This results from the singular value decomposition:

$$\mathbf{M_{acct}^{-1} = U \sum U^T} \quad (4)$$

Where, $\mathbf{\Sigma} = \text{diag}\left(\left[\sigma_1 \quad \sigma_2 \quad \sigma_3 \quad \sigma_4 \quad \sigma_5 \quad \sigma_6\right]^T\right)$ are singular values, and $\mathbf{U}$ ($\mathbf{UU^T = U^TU = I}$,) is a pose dependent unitary orthogonal matrix, $\mathbf{U}$ is a $\mathbf{6-by-6}$ unitary matrix, the matrix, $\sum$ is $\mathbf{6-by-6}$ diagonal matrix with nonnegative real numbers on the diagonal, $\mathbf{U^T}$ denotes the conjugate transpose of $\mathbf{U}$, combining (3) and (4), we then have:

$$\mathbf{U \sum U^T f_a = \ddot{\bar{I}}} \quad (5)$$

We will define new set of input and output variables $\hat{\mathbf{f}}_\mathbf{a}$, $\dot{\hat{\mathbf{X}}}$, as shown in (6) and (7):

$$\mathbf{U^T f_a = \hat{f}_a} \quad (6)$$

The new variables $\dot{\mathbf{X}}$ can be related to the actuator velocity $\dot{\mathbf{I}}$ by:

$$\mathbf{\dot{I} = U\dot{\hat{X}}} \quad (7)$$

$\dot{\mathbf{I}}$,is transformed to the generalized platform velocity $\dot{\mathbf{X}}$ by the new Jacobian matrix, $\mathbf{U}$.

Substituting $\mathbf{\dot{I} = J_{lx}\dot{X}}$ in (7) and multiplying at both sides by $\mathbf{U^T}$ we can have:

$$\mathbf{\left(U^T J_{lx}\right)\dot{X} = \dot{\hat{X}}} \quad (8)$$

The term in the bracket determines the coupling effects between DOF in task space. To numerically describe the coupling effects, equation (9) is formulated. The results of equation (9) was calculated using a configuration of a physical flight simulator motion system based on inertial and geometrical parameters; with its principal axes identical to platform coordinates. Each row of equation (9) describes decoupled modal direction in physical task space and represents the platform forces felt in relation to a unit force in any other DOF. The ratio of two elements in the rows and not the magnitude of the values are considered. Zero elements mean no coupling with any other elements (DOF). Row 1 and row 5 have similar nonzero elements at same positions but different signs that mean orthogonal directions. For row 1, the direction is positive y and negative roll, and for row 5, the direction is positive y and positive roll. Similar explanation can be given for row 2 and row 6. The physical meaning of equation (8) is that only heave and yaw can be tuned individually in task space; there exist coupling on neighboring DOFs and this influences the mass matrix evaluated along the actuator coordinates.

$$\boldsymbol{U^T J_{lq}} = \begin{bmatrix} 0.8710 & 0 & 0 & 0 & 3.8602 & 0 \\ 0 & 0.8660 & 0 & -3.86390 & 0 & 0 \\ 0 & 0 & 1.9049 & 0 & 0 & 0 \\ -0.6534 & 0 & 0 & 0 & 0.49980 & 0 \\ 0 & 0.6600 & 0 & 0.4703 & 0 & 0 \\ 0 & 0 & 0 & 0 & 0 & 3.105 \end{bmatrix} \quad 9$$

3. Dynamics of Hydraulics Servo System

For symmetric and matched servo valve and symmetrical actuator the mathematical model are given as:

$$Q_{L\,i} = K_q x_{vi} - K_c P_{Li} \tag{10}$$

$$Q_{Li} = A \cdot \dot{l}_i + k_{ce} \cdot p_{Li} + \frac{V_t}{4\beta e}\,\dot{p}_{Li} \tag{11}$$

where Q_{Li} is load flow of the i^{th} hydraulic actuator, X_{vi} is position of the i^{th} servo valve, ρ is fluid density, P_{Li} is load pressure of the i^{th} actuator, A is effective area of the piston, V_t is actuator volume, β is bulk modulus of fluid, li is the length of the i^{th} actuator K_c is flow pressure coefficient, C_{ie} is the inner leakage coefficient and K_q the flow gain. The net output force of the i^{th} actuator is given as,

$$A \cdot P_{Li} = b_c \cdot l_i + f_{ai} \tag{`12}$$

Where b_c, is the viscous damping coefficient.

Electrically operated system is faster than mechanical system; therefore, the servo valve position is equal to the valve input signal and is directly proportional to input current, then we can have

$$x_{v\,i} = u \;\; i_i = K_0 x_{vi} \;\; K_o = k_q k_a \tag{13}$$

Where, u, is the input signal, K_o is a constant, K_a is the control gain, i_i is the input current of the servo valve. To linearize the system equation and express it in form of transfer function, (11) and (12) can be rewritten in the equation (14):

$$A \cdot P_{Li} = b_c \cdot l_i s + f_{ai} \tag{14}$$

$$k_o i_i = l_i A s + \left(\frac{V_t}{4\beta_e} s + K_c \right) P_{L,i} \tag{15}$$

Equation (15) is the flow equilibrium equation of the i^{th} servo valve. Rearranging (15) the pressurization of the i^{th} actuator chamber can be described by:

$$P_{L,i} = \frac{K_o i_{u,i} - l_i A s}{\frac{Vt}{4\beta} s + K_c} \tag{17}$$

Considering the dynamic characteristics of the i^{th} actuator, we can get:

$$\sum_{i=1}^{6} \mathbf{M}_{act}^{-1}(i,j) f_{a,j} = \ddot{l}_i \tag{18}$$

Where $\mathbf{M}_{act}^{-1}(i,j)$ represents the element at the i_{th} row and j^{th} column of the inverse mass matrix in joint space, $f_{a,i}$ is a scalar describing the output force of actuator i, $\ddot{l}_i$ is a scalar denoting the acceleration of the i^{th} actuator length changes, and i,j 1,2…6.

Combining (14-18), the dynamic model of the platform in joint space can be described as:

$$\Sigma_{i=1}^{6}\mathbf{M}_{\mathbf{acct}}^{-1}(i,j)\left[\frac{K_o i_{u,i}/A - s\left(1+\frac{b_c K_c}{A^2}+\frac{b_c V_t}{4\beta A^2}s\right)l_i}{\frac{V_t}{4\beta A^2}s+\frac{K_c}{A}} = l_i s^2\right] \quad (19)$$

4. Simulation Result and Analysis

Simulation parameters were taken from physical hydraulic controlled flight simulator motion system with payload mass =13,642kg, distribution radius of upper joints points = 2.1148m, distribution radius of lower joints points =2.5170m, platform height in neutral position = 2.6519m, discharge flow rate of servo valve = 0.00064m^3/s/A, supply pressure = 12 Mpa, operational area = 0.0099m^2, viscous damping, = 8000Ns/m, hydraulics capacity = 92,564Mpa/m^3, general ratio of flow rate to pressure =6.6564x10^{-11}m^3/s/Pa.

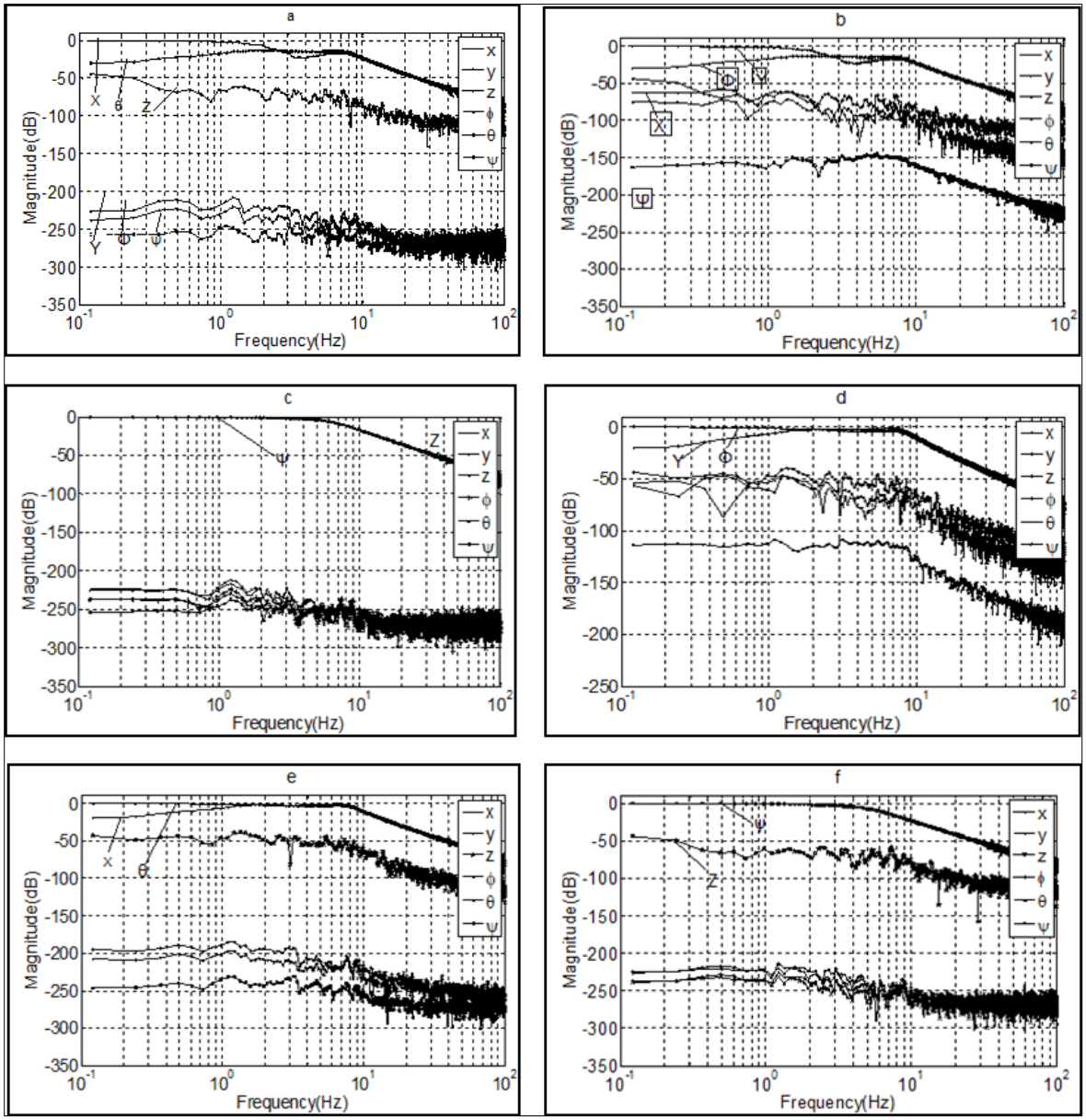

Figure 2 Coupling effects between (a) surge, (b) sway,(c) heave, (d) roll, (e) pitch, (f) yaw and other degrees of freedom

The simulation results are plotted in frequency domain and shown in Figs. 2 (a-f). The coupling effects for motion in *x* direction (surge) in Fig. 2a are heavier on pitch (θ) at 6.226Hz near the natural frequency of 6.958Hz. Also, for motion

in y direction (sway) in Fig. 2b, it is heavier on roll (ϕ), at 6.348Hz. The effects on other degrees of freedom for motion in heave *(z*) and yaw (Ψ*)* are not noticeable. This is because during motion along vertical axis, the characteristics of the leg motion are identical. Motion in roll (ϕ), pitch (θ) and the responses are given in Figs. 2d and 2e and can be explained as above. The period of 0.122hz can be regarded as the kinematic coupling effects which can be assumed negligible, the reasons given by [3], and also due to stiffness, inertia effects and level of manufacturing accuracy. The simulations results as shown below are consistent with the analytical results presented in table 1.

5. Conclusion

The coupling effects on each DOF of hydraulic controlled parallel manipulator have been presented. The analysis was based on exploitation of the properties of the joint space mass inverse matrix based on singular value decomposition. The results show the magnitude of the coupling effects between DOF. We deduced from our analysis that there are coupling between degrees of freedom due to the multi loop kinematic and closed chain spatial mechanical structure of the platform. It also shows that coupling between the degrees of freedom is dependant on frequency as the coupling effects increases with frequency and attains maximum value near the natural frequency. Simulation results in frequency domain are consistent with our theoretical analysis. The results will provide useful information to the mechanism and controller designer to evaluate at the initial stage of the design process the coupling effects on each degree of freedom and how it will affect the performance of the platform for a particular application. It will also be useful for studies on decoupling control strategies.

Compliance with ethical standards

Acknowledgments

This work was supported by 921 Manned space Project (PZJG00401D00 of China, Natural Science Foundation (NFSC-50975055) of China. The authors thank Prof. Jiang Hongzhou and Prof Han Junwei of School of Mechatronics Engineering, Harbin Institute of Technology, P. R. China for their support. They laid the foundation for this work.

Disclosure of conflict of interest

The authors declare that there is no conflict of interest.

References

[1] Huang T. Dong, CL, Liu HT, Sun, TA, Simple and visually orientated approach for type synthesis of overconstrained 1T2R parallel mechanisms. Robotica 2018, 37, 1161–1173.

[2] Chen, X.L.; Jiang, D.Y. Design, kinematics, and statics of a novel wave energy converter with parallel mechanism. Int. J. Adv. Robot. Syst. 2019, 16, 1729881419876214.

[3] Tian WJ, Shen ZQ, LP, Yin FW. A Systematic Approach for Accuracy Design of Lower-Mobility Parallel Mechanism. Robotica 2020, 38, 2173–2188.

[4] Huang T, Dong CL, Liu HT, Zhang, J.X. Conceptual design and dimensional synthesis of a novel parallel mechanism for lower-limb rehabilitation. Robotica 2019, 37, 469–480.

[5] Ogbobe PO, Zhengmao Y, Jiang H, C. Yang C, and Han J. Formulation and evaluation of coupling effects between DOF motions of hydraulically driven 6 DOF parallel manipulator', Iranian Journal of Science & Technology, Transaction of Mechanical Engineering, Vol. 35, Issue 2 - Serial Number 2, Winter 2011, Pages 143-175 DOI: 10.22099/ijstm.2011.902.

[6] Xinjian N, Chifu Y, Bowen T, Xiang LI, Han J. Modal Decoupled Dynamics Feed-Forward Active Force Control of Spatial Multi-DOF Parallel Mechanism Manipulator, Mathematical Problems in Engineering. 2019; Article ID 1835308: 13.

[7] JP Merlet. Parallel manipulators: state of the art and perspectives, Advanced Robotics. 1994; 8(6): 589-596.